

# Biophysical characterization of ovine forestomach extracellular matrix biomaterials

Evan W. Floden,<sup>1</sup> Sharif F. F. Malak,<sup>2</sup> Melissa M. Basil-Jones,<sup>3</sup> Leonardo Negron,<sup>1</sup> James N. Fisher,<sup>1</sup> Stan Lun,<sup>1</sup> Sandi G. Dempsey,<sup>1</sup> Richard G. Haverkamp,<sup>3</sup> Brian R. Ward,<sup>1</sup> Barnaby C. H. May<sup>1</sup>

<sup>1</sup>Mesyntes Limited, Lower Hutt 5040, New Zealand

<sup>2</sup>Auckland Bioengineering Institute, University of Auckland, Auckland 1010, New Zealand

<sup>3</sup>School of Engineering and Advanced Technology, Massey University, Palmerston North 4442, New Zealand

Received 13 May 2010; revised 19 July 2010; accepted 17 August 2010

Published online 4 November 2010 in Wiley Online Library (wileyonlinelibrary.com). DOI: 10.1002/jbm.b.31740

**Abstract:** Ovine forestomach matrix (OFM) is a native and functional decellularized extracellular matrix biomaterial that supports cell adhesion and proliferation and is remodeled during the course of tissue regeneration. Small angle X-ray scattering demonstrated that OFM retains a native collagen architecture ( $d$  spacing =  $63.5 \pm 0.2$  nm, orientation index =  $20^\circ$ ). The biophysical properties of OFM were further defined using ball-burst, uniaxial and suture retention testing, as well as a quantification of aqueous permeability. OFM biomaterial was relatively strong (yield stress =  $10.15 \pm 1.81$  MPa) and

elastic (modulus =  $0.044 \pm 0.009$  GPa). Lamination was used to generate new OFM-based biomaterials with a range of biophysical properties. The resultant multi-ply OFM biomaterials had suitable biophysical characteristics for clinical applications where the grafted biomaterial is under load. © 2010 Wiley Periodicals, Inc. *J Biomed Mater Res Part B: Appl Biomater* 96B: 67–75, 2011.

**Key Words:** extracellular matrix, forestomach propria submucosa, SAXS, biophysical, tissue engineering, wound healing

## INTRODUCTION

Synthetic meshes (e.g., polypropylene) have historically been used in a number of clinical applications where the graft must support load, for example, hernioplasty. However, the suitability of synthetic meshes has been under scrutiny in light of the increased infection and rejection rates associated with these materials. Consequently, there has been a move towards native biomaterials, particularly those composed of decellularized extracellular matrix (dECM), for example human acellular dermis (HAD, Alloderm<sup>®</sup>, LifeCell Corporation, NJ) and acellular small intestinal submucosa (SIS, Cook Biotech, IN). The clinical uptake of dECM-based biomaterials has been such that it is expected that these biomaterials will account for >50% of the market value of implantable meshes by 2011.<sup>1</sup> These dECM-based biomaterials are prepared from suitable source tissues that are decellularized and delaminated, typically by exposure to detergents, to yield an intact dECM.<sup>2</sup> dECM-based biomaterials retain the complexity of native tissue ECM, with an intact collagen framework consisting of structural proteins, as well as, associated cell signaling and adhesion molecules.<sup>3</sup> In this way, exogenous dECM can stimulate, support, and host cell colonization of the tissue deficit leading to regeneration. No chronic inflammatory response is observed with native dECM-based biomaterials. Instead, the observed inflammatory response is one associated with constructive

remodeling, whereby the biomaterial is degraded and replaced by a new collagenous framework as part of normal tissue remodeling.<sup>4,5</sup> Increased vascularization, as well as, reduced scar tissue and capsule formation have been noted with the use of dECM-based biomaterials following implantation. Importantly, due to their biophysical properties, either inherent or engineered, these biomaterials can physically bridge large tissue deficits to allow tension free repair of adjacent tissues and therefore replace synthetic meshes in certain clinical applications.

Biomaterials must be engineered with suitable biophysical properties to allow successful clinical use. For example, hernia grafts must withstand the load bearing stresses exerted by the contents of the abdominal cavity, retain sutures used to secure the graft, and provide sufficient elasticity to mimic natural tissue movement. Numerous technologies have been developed to modify the biophysical properties of collagen-based biomaterials to match certain clinical applications. Chemical crosslinking (e.g., 1-ethyl-3-(3-dimethylaminopropyl) carbodiimide or glutaraldehyde) is one such approach that covalently crosslinks adjacent collagen fibers to increase matrix density, strength and persistence. However, confidence in this approach has decreased due to the chronic inflammatory response that is associated with crosslinked biomaterials.<sup>4,5</sup> Other approaches have attempted to introduce new biophysical properties to collagen scaffolds

Additional Supporting Information may be found in the online version of this article.

**Correspondence to:** B. C. H. May; e-mail: barnaby.may@mesyntes.com

by combining or layering biomaterials such that the properties of the hybrid biomaterial benefits from the properties of the individual components. For example, composite biomaterials comprising urinary bladder matrix (UBM)/polyglycolic acid (PGA),<sup>6</sup> heparinized poly(vinyl alcohol)/SIS,<sup>7</sup> collagen/hydroxyapatite,<sup>8</sup> collagen/hyaluronan/chitosan,<sup>9</sup> collagen/silica,<sup>10</sup> and collagen/polypropylene,<sup>11</sup> have been reported. Although the introduction of synthetic components to tune the physical properties of collagen-based biomaterials can be effective, these advantages may be offset by the risk of introducing non-native components that may not undergo constructive remodeling. Additionally, in order for these hybrid biomaterials to properly serve as templates for regeneration they must adequately recapitulate structural features of native ECM.

As part of efforts directed at developing materials as biomimetics of native ECM, a dECM termed ovine forestomach matrix (OFM) has been developed for applications in tissue regeneration, including the treatment of chronic and acute wounds and in the form of implantable grafts for soft tissue reconstruction. OFM comprises the decellularized propria submucosa isolated from ovine forestomach tissue. Previous studies<sup>12</sup> have shown that OFM is primarily composed of collagens I and III, and retains the collagen microarchitecture of native ECM. Additional ECM-associated macromolecules (e.g., fibronectin and fibroblast growth factor basic) were also present in OFM, as were remnant basement membrane components (e.g. laminin and collagen IV) on the luminal surface and in native vascular channels. These secondary molecules, working in concert with the collagenous framework, were shown to support cell attachment, infiltration and stimulate cell differentiation.<sup>11</sup> OFM was developed as a means of addressing shortcomings with existing dECM-based biomaterials. Namely, the disease risk associated with porcine, bovine- and human-sourced dECM, the cultural and religious objections to collagens sourced from these raw materials, and the limited biophysical properties of current dECM-based biomaterials. The aim of this study was to understand the physical properties of OFM, and a series of new laminated OFM biomaterials whose properties were tunable through a process of lamination.

## MATERIALS AND METHODS

### General

OFM was prepared from ovine forestomach propria submucosa according to established procedures by Mesynthes Limited using proprietary methods.<sup>12</sup> All experiments were conducted at room temperature unless otherwise indicated. Strength testing was conducted using an Instron 5800 series electromechanical tester (Instron, MA). All samples were rehydrated in phosphate buffered saline (PBS) for at least 5 minutes prior to testing and testing was conducted within 30 minutes of rehydration. The thickness of materials was determined using a micrometer (Mitutoyo, Japan).

### Small angle X-ray scattering analysis

Lyophilized samples of OFM were characterized using small angle X-ray scattering (SAXS) according to the method

described in Basil-Jones et al.<sup>13</sup> Single SAXS images were taken from a spot  $80 \times 250 \mu\text{m}$  in size. SAXS diffraction patterns were recorded on the Australian Synchrotron SAXS/WAXS beamline, utilizing a high-intensity undulator source.

### Lamination

Thicker OFM biomaterials were created by lamination either via lyophilization, with or without additional sewing, or through adhesion of lyophilized OFM sheets using a collagen gel. All lamination procedures used a perforated stainless steel tray that allowed adequate vapor flow from the multiply laminates during lyophilization. Lamination via lyophilization proceeded as follows; a sheet of wet OFM was laid flat on a perforated stainless steel surface. Additional sheets of wet OFM were added to the top of the first to create a multilaminate stack. Care was taken to remove any air bubbles between each of the sheets. The stack of wet OFM sheets, up to eight sheets in total, was freeze dried according to proprietary procedures. The lyophilized laminates were sewn using PGA absorbable suture, 4-0 or 5-0 gauge (Foosin Medical Supplies, Shandong, China). OFM laminates were additionally created using a collagen gel prepared from powdered OFM. OFM was powdered using a spice grinder and liquid nitrogen. The powdered material was placed in PBS 10% w/v and heated at  $90^\circ\text{C}$  for 1.5 hours, then centrifuged at 4000 rpm for 20 minutes. The supernatant was shown to reversibly gel on cooling, and thus the gel was maintained at  $37^\circ\text{C}$  during application. The collagen gel was applied as a continuous layer ( $\sim 25\text{--}100 \mu\text{m}$  thick) to a single sheet of lyophilized OFM. A second layer of lyophilized OFM was applied to the layer of gel and this procedure repeated to build up a laminate of the desired thickness (up to 8-ply). Care was taken to remove any air bubbles between each of the sheets. The multi-ply stack was oven dried at  $37^\circ\text{C}$  for 24 hours prior to use during which time the collagen gel dried to adhere adjacent layers.

### Ball-burst testing

Materials were tested using an adaption to the ball burst method described in ASTM D 3787-07 "Standard Test Method for Bursting Strength of Knitted Goods, Constant-Rate-of-Travel Ball-burst Test."<sup>14</sup> A materials testing machine was equipped with a 1 kN load cell and fitted with a custom built ball-burst compression apparatus consisting of an orifice and a 25.4-mm stainless steel ball. Test samples measuring  $\sim 10 \times 10 \text{ cm}$  were centered over the orifice and clamped in place. The stainless steel ball was pushed through the test material at a constant feed rate of 305 mm/min and the compression load of failure was recorded.

### Uniaxial strength

Materials were cut with a die to "dumbbell" shaped samples with widths of 6 mm and 25 mm along the gauge length and specimen ends, respectively. The specimen ends were fixed to the grips of a materials testing machine, ensuring a grip-to-grip distance of 75 mm. The samples were tested to failure, whilst the tensile load was measured using a 100 N load cell and a constant feed-rate of 25.4 mm/min. Maximum

tangential stiffness was calculated from the slope of the load (N) versus elongation (mm curve). The load versus elongation curve was transformed to a stress (N/m<sup>2</sup>) versus strain curve, using the cross-sectional area calculated from the thickness and the width of the sample. The slope of this latter curve at its linear transition was used to calculate the modulus of elasticity, or Young's modulus (GPa).

### Suture retention test

OFM biomaterials were tested for suture retention using an adaptation of 'ANSI/AAMI VP20-1994 Guidelines for Cardiovascular Implants Vascular Prostheses Measured in Newtons. A 5 mm diameter loop of suture material (4-0, Vicryl<sup>®</sup>, Ethicon) was added to the middle of the shorter edge of OFM samples measuring 2 × 4 cm. The two ends of the suture material were knotted together using a surgeon's knot. Sutures were positioned with a bite-depth (distance from the site of the suture to the edge of the sample) of 2 mm. A 3-mm diameter round stainless steel bar was fed through the suture loops and suspended by two parallel hooks. The opposing suture-free end of the samples were held in a vice grip. The sutures were pulled through the sample at a constant feed rate of 20 mm/min and the load to failure measured with a 100 N load cell. Load at failure was defined as a 90% reduction in the observed load.

### Preparation of cross-linked OFM

OFM materials were cross-linked according to established procedures.<sup>15</sup> Briefly, sheets of hydrated OFM were prepared and cut to ~400 cm<sup>2</sup> and soaked in a solution of 0.6% *N*-hydroxysuccinimide in water (100 mL) for 5 minutes. The OFM sheets were removed and individually laid over rigid 5-mm plastic boards (400 cm<sup>2</sup>) with the luminal side facing up. A 1.15% solution of 1-ethyl-3-(3-dimethylaminopropyl)carbodiimide in water (20 mL) was added directly to the surface of the OFM sheet, ensuring that the entire surface was covered. Two similarly treated pieces of OFM were joined such that their luminal surfaces were in contact. The 'sandwich' was compressed and incubated at 37°C overnight. The 2-ply laminates were removed from the plastic sandwich, rinsed with RO H<sub>2</sub>O (3 × 250 mL), then PBS (2 × 250 mL), and finally freeze-dried using proprietary procedures. The dried materials were cut to size and tested for uniaxial strength, as described earlier.

### Permeability

Permeability indices (PI) were determined using a custom built hydrostatic permeability test rig, according to established procedures.<sup>16</sup> Test specimens measuring ~8 × 8 cm were clamped into an orifice with an internal diameter of 22 mm, such that the surface area of the test sample was 3.8 cm<sup>2</sup>. A column of distilled water was maintained with a height of 163.2 cm above the sample to achieve a pressure head of 120 mmHg. This pressure was maintained throughout the experiment. A valve that separated the water column and the sample orifice was opened at the start of the experiment allowing water to come in contact with and flow through the sample. Water passing through the sample was

collected over a period of time using a pre-weighed plastic tube. The weight of water collected (g) was converted into volume (mL), assuming density of water = 1.0 g/mL. PI were calculated using the formula; PI (120 mmHg) = volume collected (mL)/[area orifice (cm<sup>2</sup>) × time (min)]. Bovine dura was isolated from a two-year old Angus cow following slaughter (Ashurst Meat Processing, Ashurst, New Zealand). The skull was cut longitudinally and the brain tissue removed to expose the underlying dura. The dura was carefully separated from the skull and placed in sterile saline at 4°C. Dura was tested for permeability within 24 hours of harvesting.

## RESULTS

### SAXS analysis

SAXS analysis of OFM provided insight into the structure and orientation of the collagen fibrils. The periodicity in the collagen overlaps is apparent with the rings in the scattering pattern [Figure 1(A)] which, when integrated around all azimuthal angles showed distinct peaks representing the collagen overlap spacing [Figure 1(B)]. The *d* period spacing is the measurement of the collagen fibril repeating unit, termed "axial periodicity." The average *d* period was obtained from the *q* position of the peaks in Figure 1(B), and was measured in OFM as 63.5 ± 0.2 nm. Information about larger collagen structures was gained from the lower *q* regions (<0.03 Å<sup>-1</sup>). The slope at low *q* for the OFM SAXS profile [Figure 1(B)] is *q*<sup>-3.7</sup> which corresponds quite closely with a Porod's law slope (of *q*<sup>-4</sup>) and indicates that distinct boundaries exist between the collagen fibrils, which is another indicator of native collagen structure. The scattering pattern observed from the higher *q* ranges (0.04–0.1 Å<sup>-1</sup>) showed the non-isotropic nature of the collagen fibrils present in OFM [Figure 1(B)]. This non-isotropy is apparent in the significantly higher intensities of the Bragg peaks in the azimuthal region Ψ = 150°–210°, and 330°–30° compared with Ψ = 60°–120° and 240°–300° showing the orientation approximately through 0°–180°. The range of orientations in the collagen fibrils was determined by plotting the azimuthal angle versus relative intensities for a Bragg peak. A single 5° meridional arc at *q* ~ 0.06 Å<sup>-1</sup> represents only one Bragg peak, and the variation in intensity of this peak through 360° provides information on the orientation of collagen [Figure 1(C)]. OFM showed only one preferred fibril orientation that goes through ~0° and 180°. The fibril orientation index (OI), defined as the minimum angle which contains 50% of the fibrils, was calculated as 20°.

### Preparation of laminated OFM biomaterials

OFM was manufactured from ovine forestomach tissue according to established procedures<sup>12</sup> and were prepared as sheets in sizes up to approximately 40 x 40 cm. There was relatively small variation in the thickness of the material, with an average thickness of 0.25 ± 0.01 mm and a range of 0.14–0.41 mm [Figure 3 (B) and Supplementary Table 1]. Before testing samples were rehydrated in saline. Generally, the biomaterials fully rehydrated in 1–5 minutes, consistent with the reported rehydration rates of other dECMs.<sup>17</sup> Rehydration improved the handling and physical properties of OFM

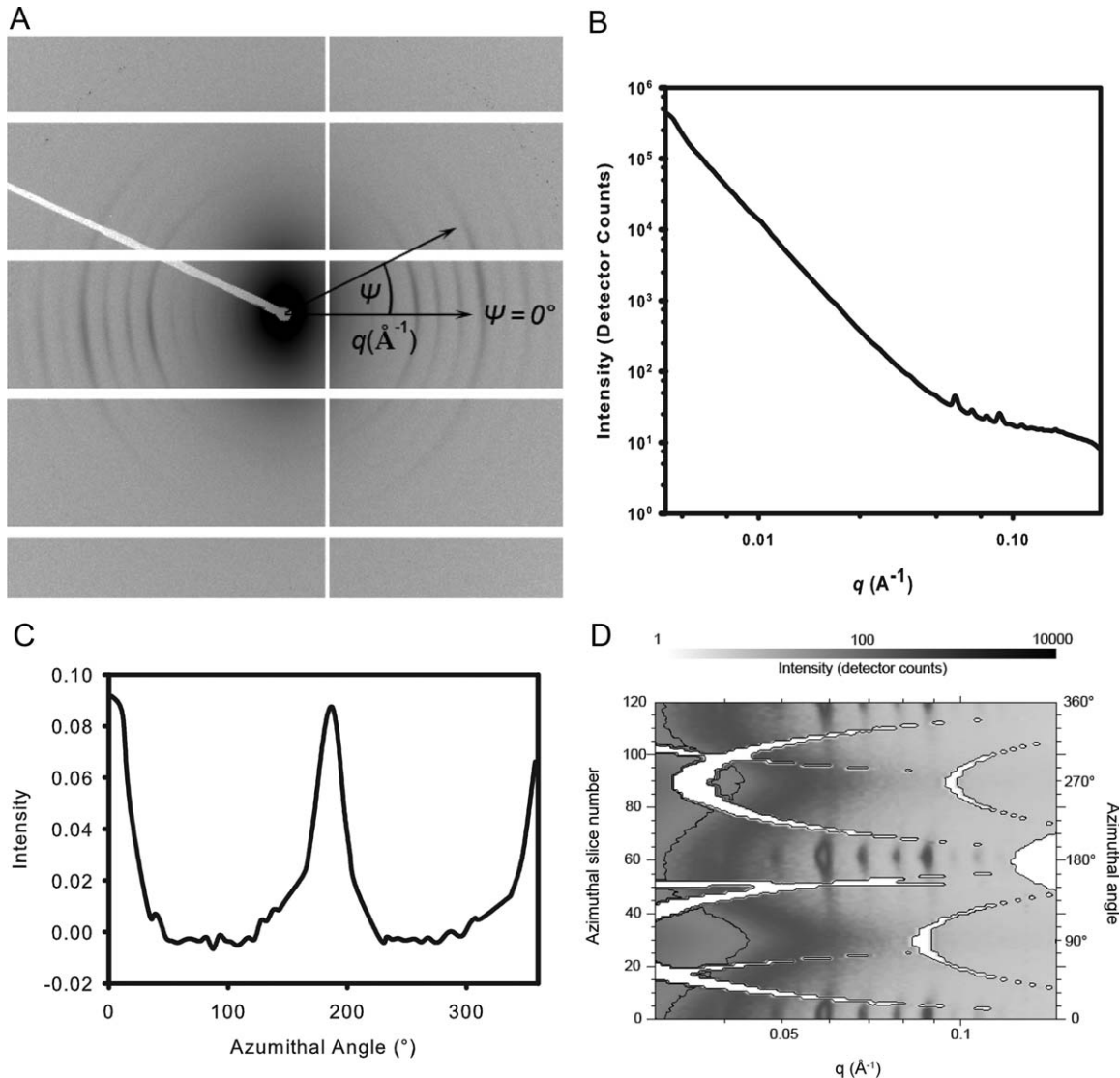


**FIGURE 1.** A. SAXS diffraction pattern for OFM. B. SAXS profile of OFM showing  $q$  versus intensity. C. Azimuthal angle plot from the Bragg peak  $q \sim 0.06 \text{ \AA}^{-1}$  with arbitrary intensity scale and offset. D. Gray shade plot of  $q$  versus azimuthal angle for OFM. The white arcs on the image represent the gaps in the detector. The dark vertical bands centered vertically on the azimuth angle of  $0^\circ$  and  $180^\circ$  are the collagen  $d$  spacing Bragg peaks. SAXS intensity is given by the gray scale.

consistent with the observations of Whitson et al.<sup>17</sup> The three methods of laminating OFM sheets all gave biomaterials of similar handling characteristics, including the ability to bunch and fold, and to be deformed. Use of lyophilization or the collagen gel adhesive did not grossly impact on the cosmetic features of the resultant OFM multilaminates. Sewing the lyophilized laminates was explored as a means of providing additional structural cohesiveness over-and-above that achieved by simply lyophilizing. In this instance, samples were sewn using a quilting pattern, comprising a series of stitch lines running perpendicular to each other [Figure 2(A)].

#### Comparison of the biophysical properties OFM biomaterials prepared with collagen gel

The OFM biomaterials were tested to the point of catastrophic failure using ball-burst, uniaxial, and suture retention

testing. In all cases, the biophysical properties were compared for a series of OFM biomaterials prepared using a collagen gel to laminate adjacent sheets. As expected, there was a dramatic increase in the strength of OFM biomaterials as the thickness was increased by adding additional sheets to produce the series of multi-ply biomaterials (up to 8-ply). The ball-burst test measured resistance to force applied equally in all directions. When considering implanted biomaterials, the ball-burst test may be considered more predictive than the uniaxial strength test, as the test load is distributed in all directions across the surface of the biomaterial. In comparison, uniaxial strength determines load at failure in one direction only. Under ball-burst testing, the 8-ply OFM biomaterial had a maximum burst strength of  $941.89 \pm 48.75 \text{ N}$ , whereas single-ply OFM was significantly weaker, with a maximum burst strength of  $92.84 \pm 12.73 \text{ N}$  [Figure 2(B) and Supplementary Table 1].



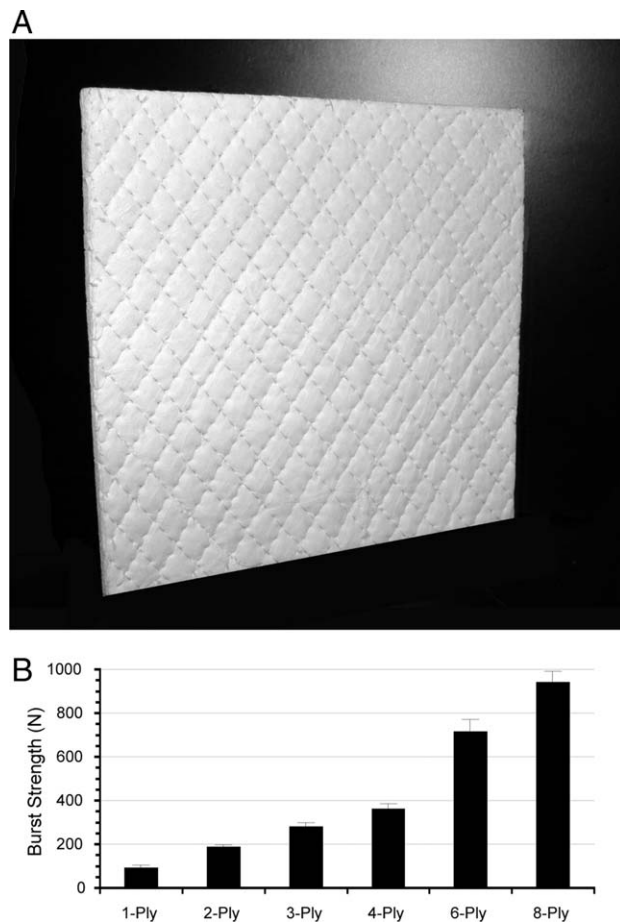


**FIGURE 2.** A. Representative image of a 6-ply OFM laminate sewn with PGA suture. B. Ball-burst strength—burst strength at failure (N) of a series of multilaminate OFM biomaterials. See Supplementary Table 1 for sample sizes ( $n$ ). Error bars represent standard error.

A comparison of the uniaxial strength properties of the OFM biomaterials is presented in Figure 3, and Supplementary Table 1. A representative bimodal stress-strain curve derived from the elongation versus force curve is shown in Figure 3(A). Stress-strain curves were characterized by a “toe region,” a transition through a linear elastic deformation region and a well-defined yield point. There was good agreement between the relative strengths of biomaterials tested under uniaxial and ball-burst methods. As expected, increasing the thickness [Figure 3(B)] of the biomaterial by increasing the lamination state significantly increased the maximum load [Figure 3(C)]. For example, the maximum load at failure of 8-ply material was  $65.13 \pm 4.37$  N, whereas the single-ply material was  $15.07 \pm 2.68$  N. Yield stress [Figure 3(F)] was determined by normalizing the maximum load to the cross sectional area of the sample. Yield stress was  $\sim 10$  MPa, irrespective of the thickness. This is to be expected given that the material composition of the laminates did not change with increasing the lamination state. There was no increase in the observed yield stress of the 2-ply ( $9.77 \pm 1.68$  MPa) material relative to the single-ply ( $10.15 \pm 1.81$  MPa) material suggesting that

the OFM determined the strength of the biomaterial rather than the collagen gel used during lamination. Lamination did not increase the maximum elongation ( $\sim 20$  mm), but the maximum tangential stiffness increased between the single- and multi-ply laminates [Figure 3(D)]. The modulus of elasticity (Young’s modulus) is an intrinsic property and describes the tendency of a material to be deformed elastically. The modulus increased between the single and multi-ply biomaterials [Figure 3(C)]. For example, the modulus of elasticity of the single-ply material was  $0.044 \pm 0.009$  GPa, whereas the 8-ply material was  $0.085 \pm 0.006$  GPa. The observed increase in the modulus and the increase in the maximum tangential stiffness suggest that the thicker biomaterials (e.g. 6- and 8-ply) prepared with collagen gel would be less elastic than thinner OFM biomaterials laminated using this approach.

Suture retention strength measures a material’s resistance to suture pull-out under uniaxial load. Suture retention strength increased relative to the thickness of the material. For example, the maximum load at failure of the single-ply and 8-ply laminates were  $5.91 \pm 0.60$  N and  $16.85 \pm 2.46$  N, respectively (Supplementary Table I). It was possible to normalize the suture retention strength to the thickness of the biomaterial (Supplementary Table 1). Normalized suture retention did not change with the increasing thickness of the laminated biomaterials.

#### Comparison of laminated OFM biomaterials

The 6-Ply OFM laminated biomaterials were created by either lyophilization, sewing a lyophilized laminate, or by use of a collagen gel to bond adjacent lyophilized OFM sheets. Sewn laminates were prepared with either 4-0 or 5-0 gauge PGA suture material. The thickness of the 6-ply collagen gel laminated biomaterial was  $\sim 30\%$  of the other laminated 6-ply biomaterials (Table I). There were no obvious differences seen in the relative strengths of the various materials using ball-burst testing and any differences might be accounted for by the natural variations seen in the OFM biomaterial, rather than the influence of the lamination technique. Indeed, under uniaxial load the 6-ply biomaterials had essentially equivalent failure points ( $\sim 50$  N). Differences in the relative thicknesses of the laminates (Table I) meant the collagen gel laminated biomaterial had the highest yield stress ( $14.81 \pm 0.94$  MPa). Sewn laminates had a lower average modulus of elasticity ( $0.047 \pm 0.003$  and  $0.033 \pm 0.006$  GPa) relative to the other laminates tested. It was difficult to distinguish the biophysical properties of laminates sewn with either the 4-0 or 5-0 suture on the basis of uniaxial testing. This suggests that the contribution of the sutures to the biophysical properties of the corresponding biomaterials was low, which is consistent with the observations that the collagen gel did not significantly contribute to the performance characteristics of the gel laminated biomaterials, as described earlier. Alternatively, there may be little to distinguish the biophysical properties of 4-0 versus 5-0 suture material such that these two materials are essentially identical under the testing performed here.

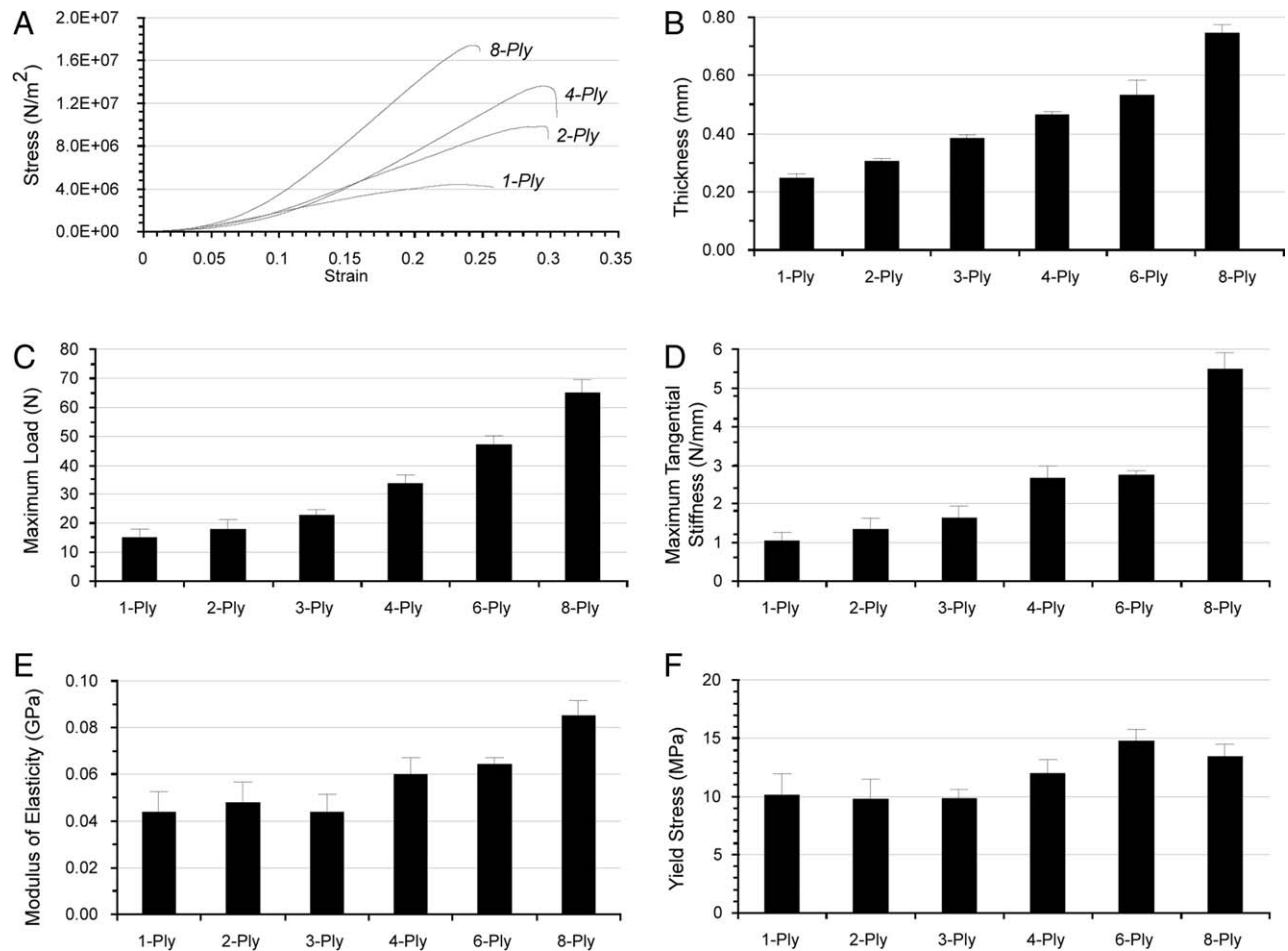


**FIGURE 3.** Uniaxial strength of multilaminate OFM biomaterials. A. Representative stress-strain curve. B. Thickness of collagen laminated OFM biomaterials. C. Maximum load at failure (N). D. Maximum tangential stiffness (N/mm). E. Young’s Modulus (GPa). F. Yield stress (MPa). See Supplementary Table 1 for sample sizes (*n*). Error bars represent standard error.

We additionally prepared cross-linked OFM biomaterials and tested these under uniaxial testing. The uniaxial strength of crosslinked OFM was reduced relative to 2-ply

laminates created using a collagen gel (yield stress,  $6.22 \pm 0.76$  and  $9.77 \pm 1.68$ , respectively). Additionally, there was a significant increase in the elasticity of the crosslinked

**TABLE I. Biophysical Properties of 6-Ply OFM Laminated Biomaterials Prepared Using a Collagen Gel, Lyophilization and by Sewing with Either 4-0 or 5-0 PGA Suture**

		6-Ply Laminate Construction			
		Collagen Gel	Lyophilized	Sewn (4-0)	Sewn (5-0)
Thickness (mm)		$0.53 \pm 0.05$ ( <i>n</i> = 6)	$1.16 \pm 0.03$ ( <i>n</i> = 6)	$1.10 \pm 0.09$	$1.26 \pm 0.10$ ( <i>n</i> = 6)
Ball-Burst	Burst strength (N)	$714.90 \pm 48.75$	$534.83 \pm 75.28$	$343.37 \pm 43.17$	$455.96 \pm 23.68$
Uniaxial Strength	Maximum load (N)	$47.31 \pm 2.99$ ( <i>n</i> = 6)	$57.93 \pm 6.05$ ( <i>n</i> = 6)	$44.72 \pm 8.18$	$43.44 \pm 6.91$ ( <i>n</i> = 6)
	Maximum elongation (mm)	$31.36 \pm 2.04$ ( <i>n</i> = 6)	$22.44 \pm 2.59$ ( <i>n</i> = 6)	$18.16 \pm 0.77$	$24.15 \pm 1.93$ ( <i>n</i> = 6)
	Maximum tangential stiffness (N/mm)	$2.77 \pm 0.10$ ( <i>n</i> = 6)	$4.90 \pm 0.89$ ( <i>n</i> = 6)	$4.16 \pm 0.52$	$3.21 \pm 0.38$ ( <i>n</i> = 6)
	Modulus of elasticity (GPa)	$0.065 \pm 0.002$ ( <i>n</i> = 6)	$0.054 \pm 0.011$ ( <i>n</i> = 6)	$0.047 \pm 0.003$	$0.033 \pm 0.006$ ( <i>n</i> = 6)
	Yield stress (Mpa)	$14.81 \pm 0.94$ ( <i>n</i> = 6)	$8.33 \pm 0.87$ ( <i>n</i> = 6)	$6.76 \pm 1.24$	$5.75 \pm 0.3$ ( <i>n</i> = 6)
Suture Retention	Maximum load (N)	$12.95 \pm 0.92$	$16.96 \pm 1.83$	$13.33 \pm 1.22$	$11.62 \pm 1.58$
	Normalized maximum load (N)	$24.43 \pm 1.73$	$14.62 \pm 1.58$	$12.12 \pm 1.11$	$10.32 \pm 1.40$

Five samples were tested, unless otherwise specified (*n*). Errors represent standard error.

**TABLE II. Permeability of Single-Ply OFM, Laminated OFM Biomaterials and Bovine Dura**

Permeability Index (mL/min/cm <sup>2</sup> )	1-Ply	2-Ply Laminate Construction			Bovine Dura
		Collagen Gel	Lyophilized	Sewn (4-0)	
Luminal→abluminal	0.0031 ± 0.0005 (n = 10)	0.0002 ± 0.0001 (n = 7)	0.0007 ± 0.0003 (n = 7)	128.57 ± 28.56 (n = 12)	0.0022 ± 0.0003 (n = 6)
Abluminal→luminal	0.0025 ± 0.0006 (n = 8)				

Single-ply OFM is anisotropic and was tested in both directions. 2-Ply OFM laminates are isotropic and were tested in one direction only. Sample sizes are as indicated (n). Errors represent standard error.

material relative to the collagen gel laminate (modulus,  $0.044 \pm 0.009$  and  $0.028 \pm 0.002$ , respectively).

### Permeability of OFM laminates

Previously, OFM was shown to be anisotropic having a distinct luminal and abluminal surface.<sup>12</sup> The luminal surface has been shown to retain remnants of the basement membrane that underlies the epithelial surface of forestomach tissue. In contrast to the smooth continuous luminal surface, the abluminal surface has a more open reticular surface. Given the differences in surface morphology of the OFM biomaterial, and the function of forestomach tissue in adsorption of nutrients from the ingesta, we investigated whether the aqueous permeability of OFM was directional. Using a custom fabricated permeability test-rig, the PI of OFM was assessed, both in the luminal→abluminal and in the abluminal→luminal directions (Table II). OFM was shown to be permeable to aqueous solutions; however, there was no statistical difference in the flow rates from either the luminal or abluminal surfaces.

To understand the effect of the various lamination techniques on the aqueous permeability of OFM laminates we quantified the permeability of various 2-ply OFM biomaterials (Table II). As expected the sewn laminate was highly permeable ( $128.57 \pm 28.6$  mL/min/cm<sup>2</sup>) owing to the needle tracks that allowed free flow of solutions across the material. The laminates prepared with either a collagen gel or via lyophilization ( $0.0002 \pm 0.0001$  and  $0.0007 \pm 0.0003$  mL/min/cm<sup>2</sup>, respectively) were significantly less permeable than the sewn laminates and were approximately half as permeable as single-ply OFM. To our knowledge, the permeability of human dura has not been established under similar testing conditions. Therefore, in an effort to identify a biologically relevant frame of reference, bovine dura was isolated and tested for aqueous permeability. Bovine and human dura are known to have similar mechanical properties,<sup>18</sup> and both comprise an especially dense arrangement of collagen fibers. Under identical testing procedures bovine dura had an aqueous permeability of  $0.0022 \pm 0.0003$  mL/min/cm<sup>2</sup> equivalent to single-ply OFM.

### DISCUSSION

Scanning electron microscopy has previously been used to confirm that the collagen matrix of OFM grossly resembles a native structure,<sup>12</sup> and we present here a SAXS analysis of the collagen arrangement at the molecular level. SAXS analysis can be used to resolve structural features of collagen

fibers, and therefore interrogate the structural integrity of collagen-containing biomaterials. As the arrangement of collagen fibers within dECM-based biomaterials largely dictates their biophysical properties, SAXS analysis is also complementary to more traditional biophysical strength testing (e.g., uniaxial or ball-burst testing). High-resolution SAXS diffraction data for dECM-based biomaterials have not previously been published, however SAXS analysis has been presented for tendon,<sup>19</sup> bone,<sup>20</sup> colonic submucosa,<sup>21</sup> and leather.<sup>13</sup> It is expected that colonic submucosa would be structurally similar to forestomach propria submucosa as both include submucosa derived from the digestive tract and contain similar collagen I/III ratios. As such, SAXS analysis of colonic submucosa provides a convenient indicator of the expected “native” collagen structure of OFM. Axial periodicity values for native collagen tissues are between 63 nm and 68 nm.<sup>21</sup> For example, the observed d period for colonic submucosa has been reported as 64.7 nm.<sup>21</sup> In comparison, the axial periodicity OFM was 63.5 nm. The close agreement between the expected axial periodicity of native submucosal ECM, as determined from colonic submucosa, and the observed axial periodicity of OFM suggests that the native fibril structure is retained in OFM. SAXS analysis revealed the OFM fibril orientation index (OI) was 20° demonstrating a highly orientated fibril network. Similarly, the fiber orientation of the dECM-based biomaterials SIS and acellular UBM have been reported using small angle lights scattering as 25°<sup>22</sup> and 46°<sup>23</sup> respectively. Therefore, there is strong evidence from SAXS and scanning electron microscopy analysis that the collagen fiber matrix in OFM is highly ordered and resembles a native collagen matrix.

Several deficiencies in the use of dECM-based biomaterials have been identified. These include laxity (bulging) due to elastic potential, seroma formation within dead space in delaminated implants, and incomplete cellular infiltration due to the thickness of the material. Being composed of decellularized human dermis, HAD is highly elastic allowing for ~50% increase in the surface area of the material.<sup>24</sup> As such, graft laxity can be problematic following the use of HAD in complex hernia and abdominal repair,<sup>24,25</sup> and it has been suggested that HAD be prestretched before implantation.<sup>26,27</sup> This is reflected in the modulus of elasticity of HAD, ~0.01 GPa.<sup>28</sup> In comparison the elasticity of OFM ( $0.044 \pm 0.009$  GPa) was shown to be comparable with the reported modulus of SIS ( $0.026 \pm 0.014$  GPa).<sup>29</sup> Biophysical testing of the OFM biomaterial additionally demonstrated that this native dECM is relatively strong (yield stress,  $10.15 \pm 1.81$  MPa) and is

consistent with the typical yield stress of implantable synthetic meshes (10 GPa or greater<sup>30</sup>). In comparison, the yield stress of UBM is  $\sim 2$  MPa.<sup>31</sup> OFM ( $92.8 \pm 12.7$  N) additionally out-performed the reported burst strength of both UBM ( $11.19 \pm 3.39$  N)<sup>31</sup> and SIS ( $20.32 \pm 1.88$  N).<sup>32</sup> One caveat to these comparisons is that the dECM-based biomaterials have not been tested in side-by-side experiments, such that the observed differences (and similarities) may reflect subtle differences in experimental conditions.

The load bearing performance characteristics of biologic implants can be improved by increasing the thickness of the graft. For example, HAD is available in a range of thicknesses ( $\sim 0.3$ – $3.3$  mm, [www.lifecell.com](http://www.lifecell.com)) reflecting the diversity of donor cadaveric dermis, whereas SIS is available in 1-, 4- and 8-ply formats. However, increasing the thickness of biologic implants to improve absolute strength can introduce additional problems. For example, thicker grafts are less likely to fully recellularize following implantation, a pathology that has been noted for both HAD and multi-ply SIS.<sup>24,33</sup> Delamination of laminated SIS has been noted following its use in hernia repair<sup>34</sup> and has been associated with intra-graft seroma between adjacent sheets of the laminated material.<sup>24</sup> Seroma formation within laminated grafts can be largely overcome by ensuring that the graft remains intact so that fluid cannot accumulate within the graft. Additionally, fenestration has been used to ensure that fluid can drain freely from within the graft and underlying tissues. To increase the absolute strength of OFM-based biomaterials various methods were explored to combine multiple layers in a process of lamination. These approaches endeavored to retain as much of the native structure and function encoded in OFM, and as such, did not explore methods that relied on chemical modification or the introduction of non-native polymers. To our knowledge, sewn dECM laminates have not previously been reported in the scientific literature and this approach offers a simple solution to modifying the biophysical properties of dECM laminated biomaterials. Chemical crosslinking has been explored as a method of improving the tensile strength of decellularized biologics, and there are a number of crosslinked biologic implants commercially available.<sup>3</sup> To understand if there were biophysical advantages to crosslinking OFM biomaterials we created 2-ply crosslinked OFM laminates using established procedures.<sup>15</sup> Chemically crosslinked OFM biomaterials demonstrated increased elasticity and reduced strength. These findings suggest that crosslinking may be associated with some denaturation of the collagen scaffold leading to a weakened matrix structure with increased elasticity, consistent with previous findings.<sup>35</sup> Given that crosslinked dECM-based biomaterials are known to illicit a foreign body response and that crosslinking does not significantly improve the biophysical performance of the OFM biomaterial, we would suggest that the applications of cross-linked OFM biomaterials are limited.

Being derived from natural tissues rather than a reconstituted collagen source, dECM-based biomaterials typically have macroscopic and microscopic differences reflecting natural variation in the source tissue. These differences are also demonstrated in the biophysical properties of the materials. For example, Sacks and Gloeckner<sup>36</sup> have shown me-

chanical anisotropy in single-ply SIS reflecting a collagen fiber alignment that runs parallel to the long axis of the intestine. Anisotropy is also evident in multi-ply SIS biomaterials and HAD.<sup>28</sup> A benefit of laminating dECM-based biomaterials is that the process of lamination has the potential to average any morphological differences seen in the materials. In this way, local biophysical differences within a sheet of material, or differences between two sheets of material are averaged out to increase homogeneity. For example, Freytes and co-workers<sup>14</sup> have overcome physical differences in the longitudinal and traverse directions of SIS by creating laminates whereby successive sheets were oriented  $45^\circ$  from each other. OFM is anisotropic having distinct luminal and abluminal surfaces.<sup>12</sup> The luminal surface arises from separation of the lamina epithelias from the propria submucosa and is characterized by protrusions resulting from remnants of the epithelial papillae. Additionally, the luminal surface is known to contain remnants of basement membrane components (e.g., laminin and collagen IV). In contrast, the abluminal surface is relatively smooth. In preparing the laminated OFM presented here, opposing layers of OFM were orientated in a luminal-luminal and abluminal-abluminal fashion, such that in all cases the exposed surfaces were the smoother abluminal face. In this way, the resulting laminated biomaterial is isotropic. It is equally possible to create OFM laminates by placing successive sheets in a luminal-abluminal orientation, such that the resultant laminates have both a luminal and abluminal surface exposed and the anisotropic characteristics of single-ply OFM are retained. Lamination also provides a route to creating larger format dECM-based biomaterials.<sup>14</sup> The ovine forestomach is a relatively large tissue source for isolating intact dECM, with sheets of up to  $40 \times 40$  cm available. However, for certain applications, lamination of overlapping sheets and subsequent sewing of the laminate, would provide a means of generating laminated biomaterials in sizes in excess of current limitations.

There is a current need for dECM-based biomaterials with biophysical properties tailored for various clinical applications. The native collagen fiber structure of OFM imparts excellent biophysical properties to this biomaterial and these properties can be extended and tuned using lamination. It has been demonstrated that it is possible to generate a range of OFM biomaterials with various thicknesses, strengths, and permeabilities. This flexibility in the OFM biomaterial opens up a range of potential applications.

#### ACKNOWLEDGMENTS

We acknowledge the Foundation for Research Science and Technology (New Zealand) MSMA0701 for funding this project. SAXS analysis was undertaken on the SAXS/WAXS beamline at the Australian Synchrotron, Victoria, Australia.

Author Disclosure: E.W.F., S.L., B.R.W., and B.C.H.M. are shareholders of Mesynthes Limited.

#### REFERENCES

1. US Markets for Soft Tissue Repair 2008: Millenium Research Group.
2. Gilbert TW, Sellaro TL, Badylak SF. Decellularization of tissues and organs. *Biomaterials* 2006;27:3675–3683.



3. Badylak SF, Freytes DO, Gilbert TW. Extracellular matrix as a biological scaffold material: Structure and function. *Acta Biomater* 2009;5:1-13.
4. Badylak SF, Gilbert TW. Immune response to biologic scaffold materials. *Semin Immunol* 2008;20:109-116.
5. Valentin JE, Stewart-Akers AM, Gilbert TW, Badylak SF. Macrophage Participation in the Degradation and Remodeling of ECM Scaffolds. *Tissue Eng Part A* 2009;15:1687-1694.
6. Eberli D, Freitas Filho L, Atala A, Yoo JJ. Composite scaffolds for the engineering of hollow organs and tissues. *Methods* 2009;47:109-115.
7. Jiang T, Wang G, Qiu J, Luo L, Zhang G. Heparinized poly(vinyl alcohol)—small intestinal submucosa composite membrane for coronary covered stents. *Biomed Mater* 2009;4:25012.
8. Al-Munajjed AA, Plunkett NA, Gleeson JP, Weber T, Jungreuthmayer C, Levingstone T, Hammer J, O'Brien FJ. Development of a biomimetic collagen-hydroxyapatite scaffold for bone tissue engineering using a SBF immersion technique. *J Biomed Mater Res B Appl Biomater* 2009;90:584-591.
9. Lin YC, Tan FJ, Marra KG, Jan SS, Liu DC. Synthesis and characterization of collagen/hyaluronan/chitosan composite sponges for potential biomedical applications. *Acta Biomater* 2009;5:2591-2600.
10. Heinemann S, Heinemann C, Bernhardt R, Reinstorf A, Nies B, Meyer M, Worch H, Hanke T. Bioactive silica-collagen composite xerogels modified by calcium phosphate phases with adjustable mechanical properties for bone replacement. *Acta Biomater* 2009;5:1979-1990.
11. van't Riet M, Burger JW, Bonthuis F, Jeekel J, Bonjer HJ. Prevention of adhesion formation to polypropylene mesh by collagen coating: A randomized controlled study in a rat model of ventral hernia repair. *Surg Endosc* 2004;18:681-685.
12. Lun S, Irvine SM, Johnson KD, Fisher NJ, Floden EW, Negron L, Dempsey SG, McLaughlin RJ, Vasudevamurthy M, Ward BR, May BC. A functional extracellular matrix biomaterial derived from ovine forestomach. *Biomaterials* 2010;31:4517-4529.
13. Basil-Jones MM, Edmonds RL, Allsop TF, Cooper SM, Holmes G, Norris GE, Cookson DJ, Kirby N, Haverkamp RG. Leather structure determination by small-angle X-ray scattering (SAXS): Cross sections of ovine and bovine leather. *J Agric Food Chem* 2010;58:5286-5291.
14. Freytes DO, Badylak SF, Webster TJ, Geddes LA, Rundell AE. Biaxial strength of multilaminated extracellular matrix scaffolds. *Biomaterials* 2004;25:2353-2361.
15. Lee JM, Edwards HHL, Pereira CA, Samii SI. Crosslinking of tissue-derived biomaterials in 1-ethyl-3-(3-dimethylaminopropyl) carbodiimide (EDC). *J Mat Sci Mat Med* 1996;7:531-541.
16. Guidoin R, King M, Marceau D, Cardou A, de la Faye D, Legendre JM, Blais P. Textile arterial prostheses: Is water permeability equivalent to porosity? *J Biomed Mater Res* 1987;21:65-87.
17. Whitson BA, Cheng BC, Kokini K, Badylak SF, Patel U, Morff R, O'Keefe CR. Multilaminar resorbable biomedical device under biaxial loading. *J Biomed Mater Res* 1998;43:277-281.
18. Runza M, Pietrabissa R, Mantero S, Albani A, Quaglini V, Contro R. Lumbar dura mater biomechanics: Experimental characterization and scanning electron microscopy observations. *Anesth Analg* 1999;88:1317-1321.
19. Sasaki N, Odajima S. Stress-strain curve and Young's modulus of a collagen molecule as determined by the X-ray diffraction technique. *J Biomech* 1996;29:655-658.
20. Cedola A, Mastrogiacomo M, Burghammer M, Komlev V, Gianoni P, Favia A, Cancedda R, Rustichelli F, Lagomarsino S. Engineered bone from bone marrow stromal cells: A structural study by an advanced x-ray microdiffraction technique. *Phys Med Biol* 2006;51:N109-N116.
21. Cameron GJ, Alberts IL, Laing JH, Wess TJ. Structure of type I and type III heterotypic collagen fibrils: An X-ray diffraction study. *J Struct Biol* 2002;137:15-22.
22. Nguyen TD, Liang R, Woo SL, Burton SD, Wu C, Almaraz A, Sacks MS, Abramowitch S. Effects of cell seeding and cyclic stretch on the fiber remodeling in an extracellular matrix-derived bioscaffold. *Tissue Eng Part A* 2009;15:957-963.
23. Gilbert TW, Wognum S, Joyce EM, Freytes DO, Sacks MS, Badylak SF. Collagen fiber alignment and biaxial mechanical behavior of porcine urinary bladder derived extracellular matrix. *Biomaterials* 2008;29:4775-4782.
24. Gupta A, Zahriya K, Mullens PL, Salmassi S, Keshishian A. Ventral herniorrhaphy: Experience with two different biosynthetic mesh materials. *Surgisis and Alloderm. Hernia* 2006;10:419-425.
25. Lin HJ, Spoerke N, Deveney C, Martindale R. Reconstruction of complex abdominal wall hernias using acellular human dermal matrix: A single institution experience. *Am J Surg* 2009;197:599-603; discussion 603.
26. Morgan AS, McIlff T, Park DL, Tsue TT, Kriet JD. Biomechanical properties of materials used in static facial suspension. *Arch Facial Plast Surg* 2004;6:308-310.
27. Vural E, McLaughlin N, Hogue WR, Suva LJ. Comparison of biomechanical properties of alloderm and enduragen as static facial sling biomaterials. *Laryngoscope* 2006;116:394-396.
28. Yoder JH, Elliott DM. Nonlinear and anisotropic tensile properties of graft materials used in soft tissue applications. *Clin Biomech (Bristol, Avon)* 2010;25:378-382.
29. Raghavan D, Kropp BP, Lin HK, Zhang Y, Cowan R, Madhally SV. Physical characteristics of small intestinal submucosa scaffolds are location-dependent. *J Biomed Mater Res A* 2005;73:90-96.
30. Barber FA, Aziz-Jacobo J. Biomechanical testing of commercially available soft-tissue augmentation materials. *Arthroscopy* 2009;25:1233-1239.
31. Freytes DO, Tullius RS, Valentin JE, Stewart-Akers AM, Badylak SF. Hydrated versus lyophilized forms of porcine extracellular matrix derived from the urinary bladder. *J Biomed Mater Res A* 2008;87:862-872.
32. Badylak JS, Voytik SL, Brightman AO, Tullius B; Purdue Research Foundation, assignee. Stomach submucosa derived tissue graft. USA. 2000.
33. Misra S, Raj PK, Tarr SM, Treat RC. Results of AlloDerm use in abdominal hernia repair. *Hernia* 2008;12:247-250.
34. Sandor M, Xu H, Connor J, Lombardi J, Harper JR, Silverman RP, McQuillan DJ. Host response to implanted porcine-derived biologic materials in a primate model of abdominal wall repair. *Tissue Eng Part A* 2008;14:2021-2031.
35. Naimark WA, Pereira CA, Tsang K, Lee JM. HMDC crosslinking of bovine pericardial tissue: A potential role of the solvent environment in the design of bioprosthetic materials. *J Mat Sci Mat Med* 1995;6:235-241.
36. Sacks MS, Gloeckner DC. Quantification of the fiber architecture and biaxial mechanical behavior of porcine intestinal submucosa. *J Biomed Mater Res* 1999;46:1-10.